JOC The Journal of Organic Chemistry

Article

pubs.acs.org/joc

Thiourea-Based Fluorescent Chemosensors for Aqueous Metal Ion Detection and Cellular Imaging

Mireille Vonlanthen,[†] Colleen M. Connelly,[‡] Alexander Deiters,[‡,§] Anthony Linden,[†] and Nathaniel S. Finney*[,†,‡]

[†]Department of Chemistry, University of Zurich, Zurich CH-8057, Switzerland

[‡]Department of Chemistry, North Carolina State University, Raleigh, North Carolina 27695, United States

[§]Department of Chemistry, University of Pittsburgh, Pittsburgh, Pennsylvania 15260, United States

Supporting Information

ABSTRACT: We describe three significant advances in the use of thioureas as reporting elements for metal-responsive fluorescent chemosensors. First, on the basis of the crystal structure of a chemosensor analogue, we provide a deeper understanding of the details of the thiourea coordination environment. Second, we describe a new generation of chemosensors with higher affinities for Zn^{2+} and Cd^{2+} than were observed for earlier probes, expanding the scope of this type of probe beyond Hg^{2+} detection. Third, we show that a thiourea-based chemosensor can be employed for fluorescence microscopy imaging of Hg^{2+} ion concentrations in living mammalian cells.

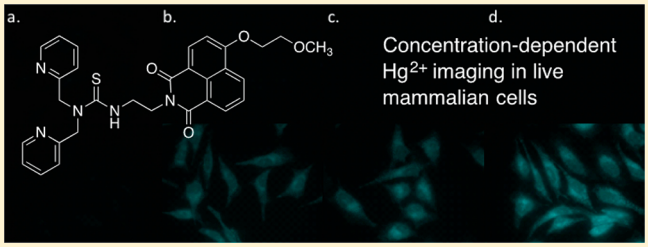

INTRODUCTION

As an analytical technique, fluorescence is remarkable for combining great sensitivity with ease of measurement. A central liability is that few analytes of interest are intrinsically fluorescent. This discrepancy has driven the development of fluorescent chemosensors, molecules that convert reversible association with a nonfluorescent analyte into a fluorescence response.[1] Fluorescent chemosensor development has been particularly effective for metallic species, and selective probes for several metal ions of biological and environmental relevance (e.g., Ca^{2+}, Zn^{2+}, and Hg^{2+}) are now available.[2−4]

The dominant approach to turning reversible metal binding into a fluorescence response is the disruption of the electronic interaction between a nitrogen atom lone pair and a proximal fluorophore via metal coordination by nitrogen.[1] Most common are the use of benzylic amine−fluorophore conjugates, in which photoinduced electron transfer (PET) from nitrogen quenches the fluorescence, and anilinic fluorophores, in which the nitrogen lone pair is engaged in the formation of an intramolecular charge transfer (ICT) excited state. In the former case, protonation or coordination suppresses the quenching and leads to enhanced emission. In the latter, protonation or coordination leads primarily to variation in the fluorophore emission wavelength, although concomitant intensity variation is not uncommon.

While these nitrogen-centric motifs have proven to be quite general,[1] reliance on nitrogen coordination for signaling possesses two characteristic shortcomings: false-positive signaling resulting from protonation (i.e., pH sensitivity) and an exclusive reliance on nitrogen coordination chemistry.

In an effort to address these issues, we have worked to develop sulfur-based functional groups as reporting elements and have recently reported the use of sulfoxides and thioureas to this end.[5,6] Building on our first generation of thiourea−naphthalimide conjugates,[6] we describe here a second generation of PET-based thiourea probes with high affinities for metal ions in aqueous media.[7,8] We find that the new chemosensors are insensitive to excess acid and can be applied in cellular imaging.

RESULTS AND DISCUSSION

First-Generation Thiourea Probes. Our validation of thioureas as PET quenchers in metal-responsive fluorescent chemosensors has so far relied on naphthalimide chromophores because of their synthetic accessibility, chemical robustness, and visible emission.[9] We have found that the fluorescent chemosensors **MePic** and **DiPic** (Figure 1) have low intrinsic quantum yields as a result of PET quenching of the fluorescence emission by the thioureas (Figure 2).[6] Emission from the pendant naphthalimide reporter can be recovered by metal ion coordination of the thiourea (Table 1) with up to 20-fold fluorescence enhancement. The addition of a large excess of H^+ (TFA) did not produce any change in the fluorescence emission of **MePic** or **DiPic**, validating our hypothesis that, in contrast to the amine-based probes described above, thioureas would provide H^+-independent signaling. Of the range of metal ions screened, the most significant fluorescence enhancements

Received: March 26, 2014
Published: June 12, 2014

   dx.doi.org/10.1021/jo500710g | J. Org. Chem. 2014, 79, 6054−6060

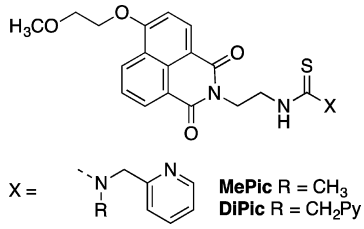

Figure 1. Fluorescent chemosensors **MePic** and **DiPic** (Py = 2-pyridyl).

were observed for the d^{10} cations Zn^{2+}, Cd^{2+}, and Hg^{2+}, although **MePic** provides a modest response to Pb^{2+} as well. Of these, Hg^{2+} was by far the most tightly bound (Table 2), and the **DiPic**·Hg^{2+} complex was found to form with $K_d \leq 15$ nM in 99:1 H_2O/CH_3CN.[6,10]

While the metal ion affinities of **MePic** and **DiPic** are similar, there is significant variation in the maximum quantum yield, which reflects details of the thiourea coordination geometry that are not yet fully understood. We have obtained a crystal structure of the 1:1 complex of $ZnCl_2$ and a truncated analogue of **DiPic** in which the fluorophore-bearing side chain is replaced by a phenyl group (Figure 3).[11] The structure reveals a near-planar thiourea and coordination of the metal center by a single pyridine unit. Notably, the coordinated zinc atom is located significantly out of the thiourea plane, with an N−C−S−Zn dihedral angle of 57.40(14)°. Bis(thiourea)zinc chloride is known to have zinc coordinated in the plane of the thiourea,[12] consistent with σ coordination by an sp^2-hybridized S atom—presumably the intrinsically preferred geometry. The observed deviation from in-plane coordination must be a consequence of geometric constraints imposed by the ring formation required for coordination of the picolyl group. From a functional point of view, these observations indicate that the coordination geometry responds strongly to structural details of the chelating group, which foreshadows the modulation of metal ion affinity and fluorescence response by ligand variation.

Consistent with the crystal structure, all of the solution-phase titrations of **MePic** and **DiPic** indicated 1:1 ligand:metal stoichiometry.[6] The Hg^{2+} affinity is sufficient to warrant evaluation of these probes in environmental samples, and it will be shown that **DiPic** is suitable for use in cellular imaging (vide infra).

A limitation of these first-generation fluorescent chemosensors is that the nitrogen atoms of the thiourea remain conjugated to and coplanar with the thiocarbonyl. As a result, the thiourea nitrogen centers are not available for coordination and only one of the distal *N*-substituents can participate in cooperative metal binding with the thiourea, as can be seen in the crystal structure (Figure 3). This accounts for the relatively low affinity observed for Zn^{2+} despite the presence of the high-Zn^{2+}-affinity dipicolyl fragment in **DiPic** and for the similarities in the metal affinities of **MePic** and **DiPic**. In conjunction with the induced deviation from optimal thiourea coordination discussed above, overcoming this limitation clearly requires

Table 1. Values of $(I/I_0)_{max}$ and ϕ_{max} for Titrations of MePic and DiPic[a]

sensor	Zn^{2+}	Cd^{2+}	Hg^{2+}	Pb^{2+}
	Titrations in CH_3OH[b]			
MePic	20.5 (0.62)	21.7 (0.65)	19.0 (0.57)	6.3 (0.19)
DiPic	13.0 (0.65)	5.0 (0.25)	7.4 (0.37)	–[c]
	Titrations in H_2O[d]			
MePic	9.3 (0.28)	4.6 (0.14)	4.4 (0.13)	–[c]
DiPic	5.7 (0.29)	4.5 (0.23)	8.6 (0.43)	–[c]

[a] ϕ_{max} in parentheses. $\phi_{max} = \phi_0 \times (I/I_0)_{max}$, where ϕ_0(**MePic**) = 0.03 and ϕ_0(**DiPic**) = 0.05. [b] Titrations in CH_3OH at 3.3 μM chemosensor. [c] No detectable fluorescence response. [d] Titrations in 9:1 H_2O/CH_3OH at 3.3 μM chemosensor.

Table 2. Apparent $\log(K_d/M)$ for Titrations of MePic and DiPic

sensor	Zn^{2+}	Cd^{2+}	Hg^{2+}	Pb^{2+}
	Titrations in CH_3OH[a]			
MePic	−3.2	−3.2	−5.8	−2.5
DiPic	−2.9	−3.1	−6.1	–[b]
	Titrations in H_2O[c]			
MePic	−1.1	−2.1	−5.9	–[b]
DiPic	−0.9	−2.3	−6.0[d]	–[b]

[a] Titrations in CH_3OH at 3.3 μM chemosensor. [b] No detectable fluorescence response. [c] Titrations in 9:1 H_2O/CH_3OH at 3.3 μM chemosensor. [d] Lower-concentration titrations revealed that this $\log(K_d/M)$ value is at least −7.8. See ref 6.

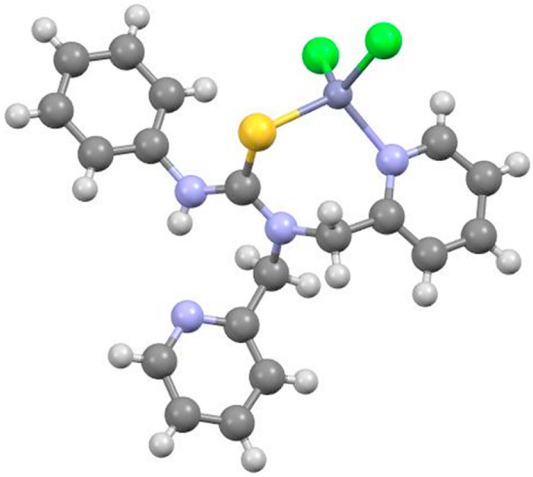

Figure 3. Molecular structure of the 1:1 complex between $ZnCl_2$ and a truncated analogue of **DiPic**.

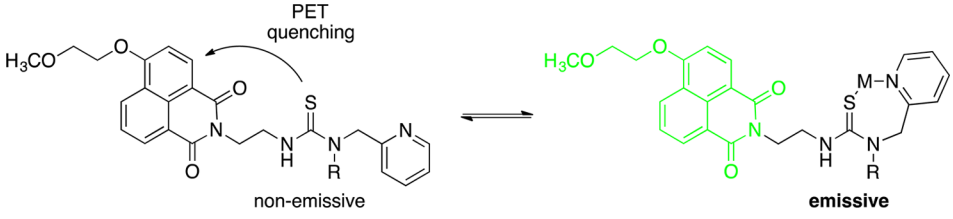

Figure 2. Fluorescent chemosensing with **MePic** and **DiPic**.

dx.doi.org/10.1021/jo500710g | J. Org. Chem. 2014, 79, 6054−6060

more extended ligand domains with a greater degree of flexibility in order to accommodate alternate coordination geometries.

Second-Generation Thiourea Probes. In order to increase the flexibility and coordination denticity of the metal-binding domains, analogues with ethylenediamine (En) spacers, **EnMePic** and **EnDiPic**, were prepared. In these molecules, the picolyl-bearing nitrogen is no longer conjugated to the thiocarbonyl, removing the associated geometric constraint and freeing the lone pair for binding (Figure 4).

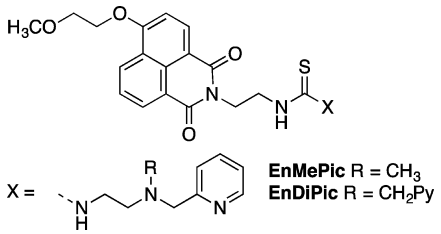

Figure 4. EnMePic and **EnDiPic**.

Mono-Boc-protected ethylenediamine was either dialkylated to form the dipicolyl derivative **1** or monoalkylated by reductive amination to give **3** (Scheme 1).[13] In the latter case, *N*-methylation provided the requisite protected diamine.[14] Following removal of the Boc group, the free amines (RNH_2) **2** and **4** were reacted with the common imidazolyl thiourea **5**, described previously,[6] to afford **EnDiPic** and **EnMePic**, respectively, in modest yields.[15]

Metal Ion Titrations. With the new probes in hand, metal ion titrations were performed in CH_3OH with Na^+, K^+, Mg^{2+}, Ca^{2+}, Ag^+, Zn^{2+}, Cd^{2+}, Hg^{2+}, and Pb^{2+}. Metal ion solutions were prepared from the corresponding metal chlorides, nitrates, or perchlorates. CH_3OH (as opposed to aqueous) solutions were chosen for initial evaluation to allow comparison with previous data and to identify binding events too weak to be observed with H_2O as the competing solvent.

Metal ion response was observed for Ag^+, the d^{10} metal cations, and Pb^{2+} but not for alkaline or alkaline-earth cations. Ag^+, Zn^{2+}, Cd^{2+}, Hg^{2+}, and Pb^{2+} titrations were then repeated in 9:1 H_2O/CH_3OH (Tables 3 and 4).[11,16] Focusing on the aqueous titrations, the magnitude of the fluorescence response, represented by $(I/I_0)_{max}$, is generally lower than in CH_3OH, and the responses to Ag^+ and Pb^{2+} are negated, as indicated by the fact that the $\log(K_d/M)$ values were too high (> -1) to be accurately determined. No fluorescence enhancement for **EnMePic** or **EnDiPic** is observed at pH as low as 5.5.[17] The response of **EnMePic** in aqueous solution is diminished relative to **MePic** (e.g., there is no response to aqueous Cd^{2+}). In contrast, the enhancements seen with **EnDiPic** are comparable or superior to those for **DiPic** and are uniformly great enough ($I/I_0 > 5$) to be potentially useful (Table 3). **EnMePic** and **EnDiPic** retain their high affinities for Hg^{2+} in 9:1 H_2O/CH_3OH, but **EnDiPic** now has pronounced affinities for Zn^{2+} and Cd^{2+} as well (Table 4), exceeding the affinity for Hg^{2+}. The $\log(K_d/M)$ values determined from the titrations are at the limit of measurement for the current reporting fluorophore, which is not bright enough to allow data acquisition below ~1 μM without repeat measurements. As a result, we think that the actual affinities are greater than the determined values, although the relative affinities are likely correct. For reasons discussed below, we have not pursued lower-concentration measurements. The stoichiometries of the Hg^{2+} and Cd^{2+} complexes are 1:1, as determined by Job plots and/or Hill coefficients.[18,19] While **EnMePic**·Zn^{2+} is also a 1:1 complex, **EnDiPic**·Zn^{2+} has 2:1 L:M stoichiometry.

There is not a clear correlation between the metal ion affinity and the magnitude of the fluorescence response. This is consistent with a complexation model in which the affinity is determined by the ethylenediamine fragment and the fluorescence response reflects the details of a second intramolecular equilibrium involving coordination of the thiourea (Figure 5). We have previously observed that thioureas have low intrinsic affinities for metal ions, allowing us to exclude direct thiourea coordination as a significant process.[6]

The affinities and intensity of fluorescence response of **EnDiPic** would appear to set the stage for applied measurements. As it turns out, although the compounds are entirely stable on the time scale of our titrations,[20] we found that **EnMePic** and **EnDiPic** degrade over the course of a day in solution and 1−2 weeks as isolated solids. The degradation leads to the formation of complex mixtures of polar material and appears to involve intramolecular cyclization coupled with

Scheme 1. Preparation of EnMePic and EnDiPic

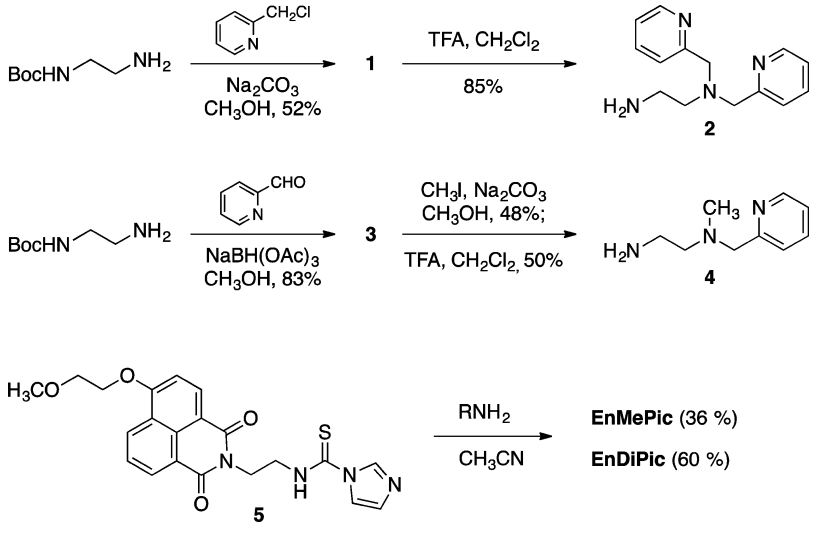

dx.doi.org/10.1021/jo500710g | J. Org. Chem. 2014, 79, 6054−6060

Table 3. Values of $(I/I_0)_{max}$ and ϕ_{max} for Titrations of EnMePic and EnDiPic[a]

sensor	Zn^{2+}	Cd^{2+}	Hg^{2+}	Ag^{+}	Pb^{2+}
			Titrations in CH_3OH[b]		
EnMePic	7.4 (0.22)	5.1 (0.15)	6.3 (0.19)	5.2 (0.16)	–[d]
EnDiPic	7.4 (0.30)	3.2 (0.13)	9.0 (0.36)	2.4 (0.10)	1.6 (0.06)
			Titrations in H_2O[c]		
EnMePic	1.9 (0.06)	–[d]	2.5 (0.08)	–[d]	–[d]
EnDiPic	11.2 (0.45)	5.3 (0.21)	7.4 (0.30)	–[d]	–[d]

[a]ϕ_{max} in parentheses. $\phi_{max} = \phi_0 \times (I/I_0)_{max}$, where ϕ_0(**EnDiPic**) = 0.04 and ϕ_0(**EnMePic**) = 0.03. [b]Titrations in CH_3OH at 3.3 μM chemosensor. [c]Titrations in 9:1 H_2O/CH_3OH at 3.3 μM chemosensor. [d]No detectable fluorescence response.

Table 4. Apparent $\log(K_d/M)$ for Titrations of EnMePic and EnDiPic

sensor	Zn^{2+}	Cd^{2+}	Hg^{2+}	Ag^{+}	Pb^{2+}
		Titrations in CH_3OH[a]			
EnMePic	−5.0	−6.9	−5.9	−5.6	–[c]
EnDiPic	−7.1	−7.0	−6.0	−5.7	−5.4
		Titrations in H_2O[b]			
EnMePic	−2.4	–[c]	−5.9	–[c]	–[c]
EnDiPic	−6.9	−7.2	−6.1	–[c]	–[c]

[a]Titrations in CH_3OH at 3.3 μM chemosensor. [b]Titrations in 9:1 H_2O/CH_3OH at 3.3 μM chemosensor. [c]No detectable fluorescence response.

dealkylation to form cyclic guanidine species. This conclusion is based on the high polarity and MS analysis of the crude degraded material; we have not yet been able to isolate purified degradation products.[21]

Cellular Assays. We were unable to deploy **EnDiPic** in cellular assays because of its instability on the assay time scale. However, we have evaluated **DiPic** as a probe for Hg^{2+} in living human cells, as Hg^{2+} is a logical starting point on the basis of the high affinity and selectivity of **DiPic** for this ion. We found that **DiPic** is sufficiently membrane-permeant to enter HeLa cells and that it allows visualization of the presence of Hg^{2+} in a concentration-dependent manner.[11] HeLa cells were incubated with **DiPic** (20 μM) overnight in standard DMEM growth medium, treated with $HgCl_2$ (200 μM) for 10 min, and examined by fluorescence imaging. In the absence of either **DiPic** or Hg^{2+} ions, no detectable fluorescence was observed, similar to that of control cells treated with DMSO only (Figure 6a–c). However, upon treatment with both **DiPic** and $HgCl_2$, a significant increase in fluorescence appeared throughout the cells but predominantly in the cytoplasm (Figure 6d). This demonstrates that the sensor **DiPic** is capable of detecting Hg^{2+} in live human cells. Moreover, **DiPic** successfully detected Hg^{2+} ions at lower concentrations of 50 and 100 μM, and the fluorescence intensity showed Hg^{2+} concentration dependence.[11]

While the practical value of imaging Hg^{2+} in biological systems may be limited,[4] these data validate the use of PET-based thiourea probes in live cells, providing a solid precedent for the design and evaluation of future thiourea probes for relevant trace thiophilic ions (e.g., Fe^{2+} or Cr^{3+}).[22]

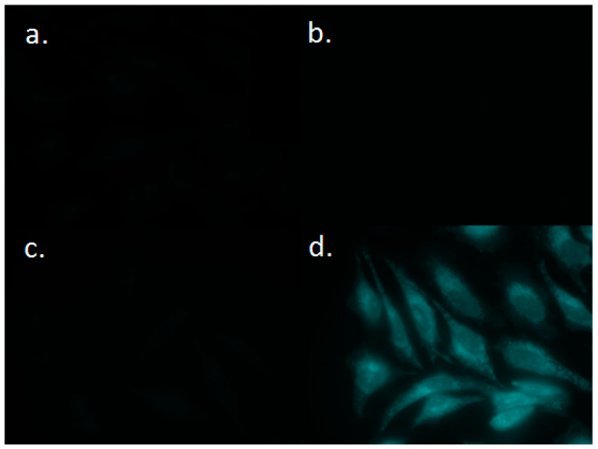

Figure 6. Fluorescence images of HeLa cells treated with **DiPic** and $HgCl_2$. (a) HeLa cells treated with a DMSO control overnight at 37 °C. (b) Cells treated with a DMSO control overnight followed by $HgCl_2$ (200 μM) for 10 min at 37 °C. (c) Cells incubated with **DiPic** (20 μM) overnight at 37 °C. (d) Cells treated with **DiPic** (20 μM) overnight followed by $HgCl_2$ (200 μM) for 10 min at 37 °C. Imaging was performed on a Zeiss Axio Observer inverted microscope using a 63× objective and excitation and emission wavelengths of 365 nm and 445/50 nm, respectively.

Next-Generation Thiourea Probes. Two important issues must be addressed in the next generation of thiourea probes: enhancement of the stability and brightness of the reporting fluorophore. The need to improve the stability is self-evident; we expect that, as observed with the first-generation fluorophores,[6] *N*-methylation of the thiourea will improve the stability. The use of more absorptive fluorophores will allow lower-concentration measurements.

CONCLUSIONS

We have shown that thiourea–naphthalimide conjugates with extended binding domains function as metal-responsive fluorescent chemosensors in aqueous media. They are capable

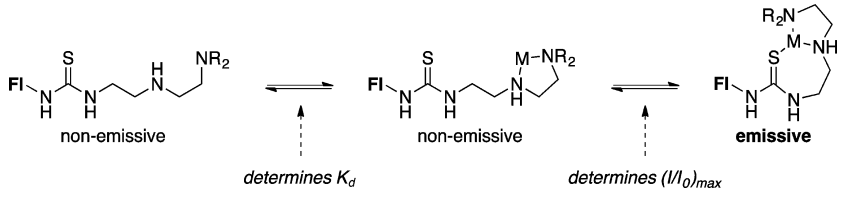

Figure 5. Proposed model for metal ion coordination (Fl = fluorophore; M = metal cation).

dx.doi.org/10.1021/jo500710g | J. Org. Chem. 2014, 79, 6054–6060

of providing a useful ($I/I_0 > 5$) turn-on response to Zn^{2+}, Cd^{2+}, and Hg^{2+} with at least high-nanomolar sensitivity. In parallel, a previously reported thiourea has been shown to be a viable optical imaging agent for Hg^{2+} in live cells. Sufficient structural understanding has been attained to allow the design of the next generation of improved thiourea-based fluorescent chemosensors, which should exhibit enhanced stability and improved measurement sensitivity and be suitable for environmental and further cellular applications.

EXPERIMENTAL SECTION

General Notes. Imidazolyl thiourea **5**, **DiPic**, and **MePic** were prepared as previously described.[6] All of the other reagents were used as received. Synthetic procedures were carried out under an inert atmosphere in dry solvent using standard Schlenk techniques, unless otherwise noted. Flash chromatographic purification was performed using silica gel Merck 60 (particle size 0.040−0.063 mm) packed in glass columns; the eluting solvent for each purification was determined by thin-layer chromatography (TLC). Analytical TLC was performed using Merck TLC silica gel 60 F254 or Macherey−Nagel POLYGRAM ALOX N/UV254.

^{1}H NMR chemical shifts are reported in parts per million relative to the solvent residual peak ($CDCl_3$, 7.26 ppm). Multiplicities are given as s (singlet), d (doublet), t (triplet), q (quartet), dd (doublet of doublets), or m (multiplet), and the coupling constants (J) are given in hertz. ^{13}C NMR chemical shifts are reported relative to the solvent residual peak ($CDCl_3$, 77.0 ppm). HRMS data were acquired on a UHPLC-HR-MS QTOF instrument with an ESI source. All of the synthetic products were noncrystalline (oils or sticky solids), precluding melting point determinations. Fluorescence measurements were carried out in spectroscopic grade CH_3OH using 450 W xenon lamp excitation with 1 nm excitation and 1 nm emission slit widths. Emission spectra were obtained by excitation at the longest-wavelength absorption maxima. For extinction coefficient determinations, four independent solutions with different concentrations were prepared, with absorption between 0.04 and 0.10 AU. The values of ε were calculated by linear least-squares fitting of plots of A versus concentration. All of the fits gave R^2 values of ≥0.98. The quantum yields for **EnMePic** and **EnDiPic** were determined by standard methods[11,23] using anthracene (ϕ = 0.30) in CH_3OH.[24] The samples were diluted to optical transparency ($A \leq 0.05$), and the integrated emission intensity was compared to that of an isoabsorptive solution of the standard in degassed solvent. Metal ion titrations were performed as previously described using metal solutions prepared with spectroscopic grade CH_3OH or unbuffered, purified H_2O.[6]

Synthetic Procedures. *N,N-Bis(2-picolyl)-N′-Boc-ethylenediamine (**1**).* 2-Chloromethylpyridine hydrochloride (451 mg, 2.75 mmol) and Na_2CO_3 (530 mg, 5.00 mmol) were added to a solution of *N*-Boc-1,2-diaminoethane (200 mg, 1.25 mmol) in methanol (20 mL), and the reaction mixture was heated to reflux for 48 h. A 2 N solution of NaOH (20 mL) was added, and the product was extracted with dichloromethane. The organic phase was washed with brine, dried over $MgSO_4$, and concentrated under vacuum. The crude product was purified by column chromatography (Al_2O_3; eluent: hexanes/CH_2Cl_2, 1:1 → CH_2Cl_2/MeOH, 99:1) to give the product as a brown-yellow oil (220 mg, 52%). The spectroscopic data were consistent with those previously reported.[13]

^{1}H NMR (δ ppm, 400 MHz, $CDCl_3$): 8.55 (ddd, 2H, J = 4.9, J = 1.8, J = 0.9), 7.64 (td, 2H, J = 7.6, J = 1.8), 7.43 (d, 2H, J = 7.8), 7.16 (ddd, 2H, J = 7.5, J = 4.9, J = 1.2), 5.80 (s, 1H), 3.89 (s, 4H), 3.25−3.22 (m, 2H), 2.75−2.72 (m, 2H), 1.44 (s, 9H). ^{13}C NMR (δ ppm, 125 MHz, $CDCl_3$): 159.2 (2), 156.2, 149.1 (2), 136.5 (2), 123.2 (2), 122.1 (2), 78.8, 60.2 (2), 53.5, 38.5, 28.5 (3). HRMS-ESI: calcd for $C_{19}H_{27}N_4O_2$ $[M + H]^+$ 343.21333, found 343.21285; calcd for $C_{19}H_{26}N_4NaO_2$ $[M + Na]^+$ 365.19510, found 365.19480. R_f (CH_2Cl_2/MeOH, 99:1): 0.2.

*N,N-Bis(2-picolyl)ethylenediamine (**2**).* **1** (80 mg, 0.23 mmol) was cooled to 0 °C in CH_2Cl_2 (2 mL), and trifluoroacetic acid (660 mg, 5.85 mmol) was added. The mixture was allowed to warm to room temperature and stirred for 2 h, and then 2 N NaOH(aq) was added. The aqueous phase extracted with CH_2Cl_2, and the combined organic fractions were dried over $MgSO_4$ and concentrated. **2** was obtained without purification as a yellow oil (48 mg, 85%). The spectroscopic data were consistent with those previously reported.[13]

^{1}H NMR (δ ppm, 400 MHz, $CDCl_3$): 8.54 (dd, 2H, J = 4.9, J = 1.3), 7.65 (td, 2H, J = 7.7, J = 1.8), 7.48 (d, 2H, J = 7.8), 7.15 (ddd, 2H, J = 7.4, J = 4.9, J = 1.2), 3.86 (s, 4H), 2.82 (t, 2H, J = 6.0), 2.69 (t, 2H, J = 6.0). ^{13}C NMR (δ ppm, 100 MHz, $CDCl_3$): 159.5 (2), 149.1 (2), 136.5 (2), 123.0 (2), 122.1 (2), 60.5 (2), 56.3, 39.3. HRMS-ESI: calcd for $C_{14}H_{19}N_4$ $[M + H]^+$ 243.16020, found 243.16045.

*4-(2-Methoxyethoxy)-N-(ethyl-1-(2-(bis(pyridin-2-ylmethyl)-amino)ethyl) thiourea)naphthalimide (**EnDiPic**).* **5** (53 mg, 0.12 mmol), acetonitrile (5 mL), and **2** (30 mg, 0.12 mmol) were combined in CH_3CN (5 mL), and the mixture was stirred for 2 h at reflux. After removal of the solvent, the crude product was purified by column chromatography (Al_2O_3; CH_2Cl_2 → CH_2Cl_2/MeOH, 99:1) to give the product **EnDiPic** (45 mg, 60%) as a yellow solid.

^{1}H NMR (δ ppm, 400 MHz, $CDCl_3$): 8.64 (dd, 1H, J = 1.6, J = 8.4), 8.59 (dd, 1H, J = 1.2, J = 7.3), 8.57−8.56 (m, 2H), 8.54 (d, 1H, J = 8.3), 7.71 (dd, 1H, J = 7.3, J = 8.4), 7.59 (dt, 2H, J = 1.8, J = 7.6), 7.35−7.33 (m, 2H), 7.12−7.09 (m, 2H), 7.04 (d, 1H, J = 8.3), 4.50−4.48 (m, 2H), 4.45−4.43 (m, 2H), 3.96−3.93 (m, 4H), 3.85 (s, 4H), 3.53 (s, 3H), 2.82 (t, 2H, J = 5.6). ^{13}C NMR (δ ppm, 100 MHz, $CDCl_3$): 181.9, 165.4, 164.8, 160.6, 159.0 (2), 149.3 (2), 136.7 (2), 134.0, 132.1, 129.7, 129.5, 126.2, 123.8, 123.3 (2), 122.3 (2), 122.1, 114.9, 106.3, 70.8, 68.7, 59.9, 59.6, 52.3, 43.0, 39.2. HRMS-ESI: calcd for $C_{32}H_{34}N_6O_4S$ $[M + H]^+$ 599.24350, found 599.24344; calcd for $C_{32}H_{33}N_6NaO_4S$ $[M + Na]^+$ 621.22545, found 621.22522. R_f (Al_2O_3; CH_2Cl_2/MeOH, 99.5:0.5): 0.25.

*N-(2-Picolyl)-N′-Boc-ethylenediamine (**3**).* *N*-Boc-1,2-diaminoethane (627 mg, 3.92 mmol) was dissolved in methanol (15 mL), and pyridine-2-carboxaldehyde (350 mg, 3.27 mmol) was added at 0 °C, and the reaction mixture was stirred at room temperature for 3 h. Sodium triacetoxyborohydride (970 mg, 4.57 mmol) was added, and the reaction mixture was stirred overnight. The solvent was removed under vacuum, and the residue was treated with saturated Na_2CO_3. The product was extracted with CH_2Cl_2, and the organic phase was dried over $MgSO_4$ and concentrated under vacuum. **3** was obtained as a brown oil (680 mg, 83%) in sufficient purity for use in the subsequent step. The spectroscopic data were consistent with those previously reported.[14]

^{1}H NMR (δ ppm, 400 MHz, $CDCl_3$): 8.56 (dd, 1H, J = 5.0, J = 1.2), 7.65 (td, 1H, J = 7.7, J = 1.8), 7.29 (d, 1H, J = 7.8 Hz), 7.18 (ddd, 1H, J = 7.5, J = 4.9, J = 1.1), 5.17 (s, 1H), 3.93 (s, 2H), 3.39−3.36 (m, 2H), 2.82−2.80 (m, 2H), 1.44 (s, 9H). ^{13}C NMR (δ ppm, 125 MHz, $CDCl_3$): 158.9, 156.2, 149.4, 136.6, 122.4, 122.2, 79.2, 54.5, 48.8, 40.2, 28.4 (3). R_f (Al_2O_3; CH_2Cl_2/MeOH, 99.5:0.5): 0.11.

*N-Methyl-N-(2-picolyl)-N′-Boc-ethylenediamine (Boc-Protected **4**).* Iodomethane (34 mg, 0.239 mmol) and sodium carbonate (85 mg, 0.80 mmol) were added to a solution of **3** (50 mg, 0.20 mmol) in CH_3OH (20 mL), and the reaction mixture was heated to reflux for 72 h. The solvent was concentrated under vacuum, and the crude product was purified by column chromatography (Al_2O_3; eluent: CH_2Cl_2). The product was obtained as a light-yellow oil (25 mg, 48%).

^{1}H NMR (δ ppm, 400 MHz, $CDCl_3$): 8.57−8.55 (m, 1H), 7.67 (td, 1H, J = 7.7, J = 1.8), 7.38 (d, 1H, J = 7.9), 7.18 (dd, 1H, J = 7.4, J = 3.0), 3.71 (s, 2H), 3.27−3.25 (m, 2H), 2.59−2.57 (m, 2H), 2.32 (s, 3H), 1.45 (s, 9H). ^{13}C NMR (δ ppm, 125 MHz, $CDCl_3$): 159.0, 156.2, 149.3, 136.6, 123.2, 122.2, 79.2, 63.8, 56.5, 42.4, 38.2, 38.6 (3). HRMS-ESI: calcd for $C_{14}H_{24}N_3O_2$ $[M + H]^+$ 266.1863, found 266.1864. R_f (Al_2O_3; CH_2Cl_2): 0.31.

*N-Methyl-N-(2-picolyl)ethylenediamine (**4**).* *N*-Methyl-*N*-(2-picolyl)-*N′*-Boc-ethylenediamine (150 mg, 0.57 mmol) was cooled to 0 °C in CH_2Cl_2 (10 mL), and trifluoroacetic acid (1.61 g, 14.15 mmol) was added. The mixture was allowed to warm to room temperature and stirred for 2 h. Then 2 N NaOH(aq) was added, and the aqueous phase was extracted with CH_2Cl_2. The combined organic fractions were dried over $MgSO_4$ and concentrated. **4** was obtained without

dx.doi.org/10.1021/jo500710g | J. Org. Chem. 2014, 79, 6054−6060

purification as a yellow oil (48 mg, 50%) and used immediately in the next reaction.

^{1}H NMR (δ ppm, 400 MHz, $CDCl_3$): 8.57−8.55 (m, 1H), 7.68−7.64 (m, 1H), 7.38 (d, 1H, J = 7.9), 7.19−7.17 (m, 1H), 3.68 (s, 2H), 2.56−2.54 (m, 4H), 2.26 (s, 3H).

*4-(2-Methoxyethoxy)-N-(ethyl-1-(2-methyl(2-picolyl)amino)-ethyl)thiourea)naphthalimide (**EnMePic**).* **5** (103 mg, 0.24 mmol), acetonitrile (5 mL), and **4** (40 mg, 0.24 mmol) were combined in CH_3CN (5 mL), and the mixture was stirred for 2 h at reflux. The solvent was removed, and the crude product was purified by column chromatography (Al_2O_3; CH_2Cl_2 → CH_2Cl_2/MeOH, 99:1) to give the product **EnMePic** as a yellow solid (45 mg, 36%).

^{1}H NMR (δ ppm, 400 MHz, $CDCl_3$): 8.66−8.55 (m, 3H), 8.53 (d, 1H, J = 8.3), 7.70 (dd, 1H, J = 7.3, J = 8.4), 7.62 (td, 1H, J = 1.8, J = 7.7), 7.34 (d, 1H, J = 7.8), 7.14 (dt, J = 2.9, J = 8.1), 7.05 (d, 1H, J = 8.3), 4.57−4.36 (m, 4H), 4.01−3.81 (m, 4H), 3.73 (s, 2H), 3.52 (s, 5H), 2.71 (s, 2H), 2.31 (s, 3H). ^{13}C NMR (δ ppm, 125 MHz, $CDCl_3$): 182.0, 165.4, 164.7, 160.6 (2), 149.4, 136.8, 134.0, 132.1, 129.6, 129.6, 126.2, 123.7, 123.4, 122.4, 122.0, 114.8, 106.0, 70.8, 68.6, 63.3, 59.6, 55.4, 53.6, 42.2, 39.1. HRMS-ESI: calcd for $C_{27}H_{32}N_5O_4S$ $[M + H]^+$ 522.21695, found 522.21711. R_f (Al_2O_3; CH_2Cl_2/MeOH, 99.5:0.5): 0.25.

Cell Culture. Experiments were performed using HeLa cells (ATCC) cultured in Dulbecco's Modified Eagle Medium (DMEM) (Hyclone) supplemented with 10% fetal bovine serum (FBS) (Hyclone) and 2% penicillin/streptomycin (Mediatech) and maintained at 37 °C in a 5% CO_2 atmosphere.

Detection of Hg^{2+} Ions in Mammalian Cells. HeLa cells were passaged into an eight-well chamber slide at 10 000 cells/well and grown overnight at 37 °C. The medium was removed, and the cells were treated with either a DMSO control (1% DMSO final concentration) or **DiPic** (20 μM) in DMEM and then incubated overnight at 37 °C. The medium was removed, and the cells were washed three times with PBS (100 μL). The cells were then treated with $HgCl_2$ at 0 or 200 μM in PBS and incubated for 10 min at 37 °C. The cells were imaged for fluorescence on a Zeiss Axio Observer inverted microscope using a 63× objective and filter set 49 (excitation 365 nm, emission 445/50 nm).

■ ASSOCIATED CONTENT

Supporting Information

Representative absorbance, emission, and titration spectra; concentration-dependent Hg^{2+} imaging in HeLa cells; ORTEP for the structure in Figure 3; copies of ^{1}H and ^{13}C NMR spectra; and crystallographic data for the structure in Figure 3 (CIF). This material is available free of charge via the Internet at http://pubs.acs.org.

■ AUTHOR INFORMATION

Corresponding Author

*E-mail: nsfinney@ncsu.edu.

Notes

The authors declare no competing financial interest.

■ ACKNOWLEDGMENTS

This work was supported by the Swiss National Science Foundation, the Institute of Organic Chemistry (UZH), and a GlaxoSmithKline graduate fellowship (C.M.C.).

■ REFERENCES

(1) For representative reviews of fluorescent chemosensors and probes, see: (a) Li, X.; Gao, X.; Shi, W.; Ma, H. *Chem. Rev.* **2014**, *114*, 590−659. (b) Formica, M.; Fusi, V.; Giorgi, L.; Micheloni, M. *Coord. Chem. Rev.* **2012**, *256*, 170−192. (c) de Silva, A. P.; Uchiyama, S. *Top. Curr. Chem.* **2011**, *300*, 1−28. (d) Quang, D. T.; Kim, J. S. *Chem. Rev.* **2010**, *110*, 6280−6301. (e) Cho, D.-G.; Sessler, J. L. *Chem. Soc. Rev.* **2009**, *38*, 1647−1662. (f) Demchenko, A. P. *Introduction to Fluorescence Sensing*; Springer Science: London, 2009; Chapter 6. (g) Tsukanov, A. V.; Dubanosov, A. D.; Bren, V. A.; Minkin, V. I. *Chem. Heterocycl. Compd.* **2008**, *44*, 899−923. (h) Callan, J. F.; de Silva, A. P.; Magri, D. C. *Tetrahedron* **2005**, *61*, 8551−8588. (i) de Silva, A. P.; Gunaratne, H. Q. N.; Gunnlaugsson, T.; Huxley, A. J. M.; McCoy, C. P.; Rademacher, J. T.; Rice, T. E. *Chem. Rev.* **1997**, *97*, 1515−1566.

(2) For an overview of fluorescent probes for Ca^{2+}, see: Simpson, A. W. M. *Methods Mol. Biol.* **2013**, *937*, 3−36.

(3) For an overview of fluorescent Zn^{2+} detection, see: Huang, Z.; Lippard, S. J. *Methods Enzymol.* **2012**, *505*, 445−468.

(4) For overviews of fluorescent Hg^{2+} detection, see: (a) Kim, H. N.; Ren, W. X.; Kim, J. S.; Yoon, J. *Chem. Soc. Rev.* **2012**, *41*, 3210−3244. (b) Nolan, E. M.; Lippard, S. J. *Chem. Rev.* **2008**, *108*, 3443−3480.

(5) Kathayat, R. S.; Finney, N. S. *J. Am. Chem. Soc.* **2013**, *135*, 12612−12614.

(6) Vonlanthen, M.; Finney, N. S. *J. Org. Chem.* **2013**, *78*, 3980−3988.

(7) For reviews of anion coordination by ureas/thioureas, see: (a) Gunnlaugsson, T.; Ali, H. D. P.; Glynn, M.; Kruger, P. E.; Hussey, G. M.; Pfeffer, F. M.; Santos, C. M. G.; Tierney, J. *J. Fluoresc.* **2005**, *15*, 287−299. (b) Amendola, V.; Bonizzoni, M.; Esteban-Gomez, D.; Fabbrizzi, L.; Licchelli, M.; Sancenon, F.; Taglietti, A. *Coord. Chem. Rev.* **2006**, *250*, 1451−1470. (c) Gunnlaugsson, T.; Glynn, M.; Tocci, G. M.; Kruger, P. E.; Pfeffer, F. M. *Coord. Chem. Rev.* **2006**, *250*, 3094−3117. (d) Li, A.-F.; Wang, J.-H.; Wang, F.; Jiang, Y.-B. *Chem. Soc. Rev.* **2010**, *39*, 3729−3745. (e) Duke, R. M.; Veale, E. B.; Pfeffer, F. M.; Kruger, P. E.; Gunnlaugsson, T. *Chem. Soc. Rev.* **2010**, *39*, 3936−3953.

(8) For an early example of a PET-based chemosensor that does not rely on nitrogen, see: de Silva, A. P.; Sandanayake, K. R. A. S. *J. Chem. Soc., Chem. Commun.* **1989**, 1183−1185. For other examples, see especially ref 1i.

(9) For overviews of the versatility of naphthalimide fluorophores, see ref 7e and: Banerjee, S.; Veale, E. B.; Phelan, C. M.; Murphy, S. A.; Tocci, G. M.; Gillespie, L. J.; Frimannsson, D. O.; Kelly, J. M.; Gunnlaugsson, T. *Chem. Soc. Rev.* **2013**, *42*, 1601−1618.

(10) For reports of Hg^{2+}-responsive fluorescent chemosensors based on aminomethylanthracene thioureas, in which PET has been claimed as the operant signaling mechanism, see: (a) Profatilova, I. A.; Bumber, A. A.; Tolpygin, I. E.; Rybalkin, V. P.; Gribanova, T. N.; Mikhailov, I. E.; Bren, V. A. *Russ. J. Gen. Chem.* **2005**, *75*, 1774−1781. (b) Tolpygin, I. E.; Shepelenko, E. N.; Revinskii, Y. V.; Tsukanov, A. V.; Dubonosov, A. D.; Bren, V. A.; Minkin, V. I. *Russ. J. Gen. Chem.* **2010**, *80*, 756−770.

(11) See the Supporting Information.

(12) Kunchur, N. R.; Truter, M. R. *J. Chem. Soc.* **1958**, 3478−3484.

(13) *N*,*N*-Bis(picolyl)ethylenediamine: (a) Romary, J. K.; Barger, J. D.; Bunds, J. E. *Inorg. Chem.* **1968**, *7*, 1142−1145. By reductive amination: (b) Matouzenko, G. S.; Bousseksou, A.; Lecocq, S.; van Koningsbruggen, P. J.; Perrin, M.; Kahn, O.; Collet, A. *Inorg. Chem.* **1997**, *36*, 2975−2981. In Boc-protected form: (c) Hanaoka, K.; Kikuchi, K.; Urano, Y.; Nagano, T. *J. Chem. Soc., Perkin Trans. 2* **2001**, 1840−1843.

(14) Lim, N. C.; Ewart, C. B.; Bowen, M. L.; Ferreira, C. L.; Barta, C. A.; Adam, M. J.; Orvig, C. *Inorg. Chem.* **2008**, *47*, 1337−1345.

(15) **EnMePic**: ε = 13 800 cm^{-1} M^{-1}; ϕ = 0.03; λ_{max}^{abs} = 368 nm (longest-wavelength maximum); λ_{max}^{em} = 446 nm. **EnDiPic**: ε = 14 500 cm^{-1} M^{-1}; ϕ = 0.04; λ_{max}^{abs} = 368 nm (longest-wavelength maximum); λ_{max}^{em} = 446 nm.

(16) Binding constants were determined by nonlinear least-squares fitting of plots of emission intensity vs log[M] using the program Prism3 (Graphpad, Inc., San Diego, CA).

(17) The addition of HCl to a solution of **EnMePic** or **EnDiPic** does not produce a change in fluorescence until pH ∼5. At this point, the protonated picolylamine begins to serve as an alternate PET acceptor, and the fluorescence begins to increase. For precedent, see: de Silva, S. A.; Zavaleta, A.; Baron, D. E.; Allam, O.; Isidor, E. V.; Kashimura, N.; Percarpio, J. M. *Tetrahedron Lett.* **1997**, *38*, 2237−2240.

(18) (a) Connors, K. A. *Binding Constants*; John Wiley & Sons: New York, 1987. (b) Huang, C. Y. *Methods Enzymol.* **1982**, *87*, 509−525.
(19) Hill coefficients can provide an indication of binding stoichiometry. See: (a) Chow, C. C.; Ong, K. M.; Dougherty, E. J.; Simons, S. S., Jr. *Methods Enzymol.* **2011**, *487*, 465−483. However, this approach must be used with caution; for example, see: (b) Lissi, E.; Calderon, C.; Campos, A. *Photochem. Photobiol.* **2013**, *89*, 1413−1416.
(20) We have found that **EnMePic** and **EnDiPic** can be recovered untransformed following exposure to Zn^{2+} and Hg^{2+} for several hours in CH_3OH. This excludes the possibility that the fluorescence enhancements are the result of desulfurization of the thiourea. The addition of chelating agents (EDTA or dipicolylamine) reverses the observed fluorescence enhancements.
(21) There is a precedent for metal-ion-induced cyclization of *N*-(*β*-aminoethyl)-*N*′-acylthioureas to form cyclic guanidines in the context of chemodosimeters, in which a *β*-amino NH serves as the nucleophile (see refs 1a and 1d). We had anticipated that the absence of a free *β*-NH would suppress such cyclization.
(22) For a review of Fe^{3+}-responsive fluorescent chemosensors, see: (a) Sahoo, S. K.; Sharma, D.; Bera, R. K.; Crisponi, G.; Callan, J. F. *Chem. Soc. Rev.* **2012**, *41*, 7195−7227. For recent examples of Cr^{3+}-selective fluorescent chemosensors, see: (b) Goswami, S.; Das, A. K.; Maity, A. K.; Manna, A.; Aich, K.; Maity, S.; Saha, P.; Mandal, T. K. *Dalton Trans.* **2014**, *43*, 231−239. (c) Goswami, S.; Aich, K.; Das, S.; Das, A. K.; Sarkar, D.; Panja, S.; Mondal, T. K.; Mukhopadhyay, S. *Chem. Commun.* **2013**, *49*, 10739−10741. (d) Zhao, M.; Ma, L.; Zhang, M.; Cao, W.; Yang, L.; Ma, L.-J. *Spectrochim. Acta, Part A* **2013**, *116*, 460−465.
(23) Lakowicz, J. R. *Principles of Fluorescence Spectroscopy*; Springer: New York, 2006.
(24) Berlman, B. I. *Handbook of Fluorescent Spectra*; Academic Press: New York, 1965.